frontiers in Marine Science

ORIGINAL RESEARCH
published: 05 November 2019
doi: 10.3389/fmars.2019.00662

Simulating Bleaching: Long-Term Adaptation to the Dark Reveals Phenotypic Plasticity of the Mediterranean Sea Coral *Oculina patagonica*

*Tal Zaquin[1], Paul Zaslansky[2], Iddo Pinkas[3] and Tali Mass[1]**

[1] Department of Marine Biology, The Leon H. Charney School of Marine Sciences, University of Haifa, Haifa, Israel, [2] Department for Operative and Preventive Dentistry, Charité Dental School – Charité – Universitätsmedizin Berlin, Berlin, Germany, [3] Department of Chemical Research Support, Weizmann Institute of Science, Rehovot, Israel

OPEN ACCESS

Edited by:
Noga Stambler, Bar-Ilan University, Israel

Reviewed by:
Esti Kramarsky-Winter, Ben-Gurion University of the Negev, Israel
Anthony William Larkum, University of Technology Sydney, Australia

***Correspondence:**
Tali Mass
tmass@univ.haifa.ac.il

Specialty section:
This article was submitted to Coral Reef Research, a section of the journal Frontiers in Marine Science

Received: *04 July 2019*
Accepted: *10 October 2019*
Published: *05 November 2019*

Citation:
Zaquin T, Zaslansky P, Pinkas I and Mass T (2019) Simulating Bleaching: Long-Term Adaptation to the Dark Reveals Phenotypic Plasticity of the Mediterranean Sea Coral Oculina patagonica. Front. Mar. Sci. 6:662. doi: 10.3389/fmars.2019.00662

The Eastern Mediterranean Sea scleractinian *Oculina patagonica*, demonstrates high resilience to repeated seasonal bleaching events, a trait potentially allowing the species to survive through a radically changing climate. However, the physiological and morphological contributors that make this plasticity of *O. patagonica* possible are poorly understood. Here we use a long-term *in vitro* induced bleaching experiment where colonies were reared in a dark environment to examine how *O. patagonica* colonies can survive without endosymbionts. We assessed the physiological, morphological and genetic adaptations that accompany our controlled bleaching. Measurements reveal changes to respiration and calcification rates both at 3 and 12 months following the initiation of the darkness experiment, coupled with corresponding macromorphology traits. Upon placing in the dark environment, *O. patagonica* begins the bleaching process while demonstrating acclimation in which the coral appears to divert its energy to survival resulting in the expulsion of the Symbiodiniaceae population. In addition, the coenosarc exhibits degradation where the coral transforms from a colonial living to a solitary one. Once bleached, we observe adaptation by the solitary polyps characterized by a lower respiration rate yet, regaining their calcification activity and are continuing gametogenesis. However, under bleaching conditions, the newly formed skeletons differ substantially from non-bleached colonies, clearly suggesting an environmental influence on the skeleton morphology. Overall, our study reveals that *O. patagonica* shows phenotypic plasticity allowing the species to withstand losing their beneficial endosymbionts so as to prosper as a solitary coral. The mechanisms used by this highly resilient coral may provide clues to what corals may require to be able to adapt to life without photosynthetic symbionts.

Keywords: coral bleaching, translocation, stress response genes, transcriptome, SEM-EDS, micro-Raman, micro-CT, phenotypic plasticity

INTRODUCTION

Stony coral species (order Scleractinia) have a mutual endosymbiotic association with photosynthetic dinoflagellate, commonly known as zooxanthellae (family Symbiodiniaceae) (Trench, 1979; Stat et al., 2006; Venn et al., 2008). Coral bleaching, which is the partial or full loss by the coral host of the zooxanthellae population, is a result of a usually localized natural occurrence (Lough and van Oppen, 2018). However, in recent decades, bleaching occurs in a much larger scale with globally catastrophic implication related to a range of anthropogenic-induced environmental changes such as elevated temperature events, acidification, and overexposure to radiation which has coined the term "global mass bleaching" (Glynn, 1983; Baker et al., 2008; Bessell-Browne et al., 2017). The loss of the symbiosis can lead to starvation of the host as the zooxanthellae provide up to 100% of the coral daily metabolic requirements (Davies, 1984; Falkowski et al., 1984). Bleached corals are more susceptible to diseases, have a lower metabolic turnover and exhibit a decrease in respiration and calcification rates (Glynn, 1993; Høegh-Guldberg, 1999; Baker et al., 2008). The possibility of coral recovering from mass bleaching events is widely investigated, and usually requires successful larval recruitment, or a clade shift of the endosymbiont algae (Roberts et al., 1997; Høegh-Guldberg, 1999; Rodrigues and Grottoli, 2007; Graham et al., 2015; Schoepf et al., 2015; Berkelmans, 2018; Hughes et al., 2019). Annual severe bleaching events are predicted to occur worldwide more frequently and on a larger spatial scale. Such phenomena may put more than 90% of all coral reefs at risk by the end of the century because the organisms require several seasons to be able to adapt to the changing environment (Frieler et al., 2013; Grottoli et al., 2014; Schoepf et al., 2015; Donner et al., 2018).

Although rare, certain coral species display a repeated natural seasonal bleaching pattern, which does not result in massive coral mortality; such repeated bleaching occurs for example in the mesophotic tropical coral *Stylophora pistillata* (Nir et al., 2014) and the temperate scleractinian coral Mediterranean *Oculina patagonica* (Shenkar et al., 2005). Curiously, research has shown that not only do these corals survive such bleaching events, often they actually prosper, as demonstrated by continued gametogenesis in *O. patagonica* (Armoza-Zvuloni et al., 2011).

Studies concentrating on the loss of the symbionts-host relationship usually focus on reef-building corals (Dubinsky and Stambler, 2011; Tolleter et al., 2013; van Oppen and Lough, 2018) as they are among the most important providers of ecological goods and services (Moberg and Folke, 1999). However, studying thriving species of corals from other habitats might help us understand the mechanisms that allow these corals to thrive. Such information may be useful when dealing with endangered species of corals. One of the most researched non-tropical coral species is *O. patagonica*, a common and highly tolerant Mediterranean coral, presenting both a zooxanthellate and azooxanthellate phenotype that can be found in diverse habitats including crevices, caves and disturbed sites (Fine et al., 2001). However, comparison between different habitats and phenotype is beyond the scope of this study. In the present work we are examining the stages involved in the acclimation and eventual adaptation of the zooxanthellate coral to life without photosynthesizing endosymbionts.

MATERIALS AND METHODS

Study Organism and Experimental Design

Eight *O. patagonica* colonies were collected from Sdot-Yam, Israel (32°29′25.3″N 34°53′17.6″E) in July 2017 under a special permit from the Israeli Natural Parks Authority. The samples were collected at depths of 4–6 m and immediately transported to a controlled environment aquarium system, at the Leon H. Charny School of Marine Sciences in the University of Haifa. The corals were allowed to recover for 2 weeks under simulated ambient conditions, and thereafter each of the colonies were further divided into six fragments (∼2 cm diameter). A total of 24 fragments (three from each colony), were kept in a closed-circuit aquarium system with the same ambient light conditions as those of the Sdot Yam waterfront (named "Amb"), and 24 fragments were placed in a completely dark system (named "Dark") for 12 months and more as described below. Except for light parameters, both systems were maintained with the same physical and chemical water values (temperature, salinity, pH, calcium, magnesium, phosphate and nitrate), replicating the Eastern Mediterranean Sea conditions (Krom and Suari, 2015) that were controlled biweekly. Water changes of 10% were performed on a weekly basis for all aquarium systems using artificial seawater (Red Sea Salt, Red Sea Ltd.) and all corals were fed identical food twice a week (Microvore, Brightwell® aquatics, United States).

During the entire period of the experiment, observations of macromorphology of the living colonies were conducted continuously, with a stereomicroscope (SMZ800N, Nikon, Japan). To study the acclimation of *O. patagonica* to the a dark environment, fragments were sampled at 3 ("Amb3" and "Dark3"), 12 ("Amb12" and "Dark12") and 18 ("Amb18" and "Dark18") months past the initial placement in the dark. Fragments were treated according to the following protocols and sampled according to the workflow scheme (**Figure 1**).

Photosynthesis Efficiency

Three fragments from Amb3/Dark3 and Amb12/Dark12 were dark incubated for 30 min. Thereafter, photosynthesis efficiency was measured to determine the ratio of variable fluorescence (Fv) to maximum fluorescence (Fm) denoted Fv/Fm using the Maxi Imaging-PAM (Walz, Germany) (Ralph et al., 1999). After the measurements, all fragments were returned to their respective aquaria.

Dark Respiration Rates

Other Amb3/Dark3 and Amb12/Dark12 fragments ($n = 3$) were dark incubated for 3 h. Each fragment was then placed in a sealed sterile polypropylene specimen cup (Miniplast, Israel) filled with artificial seawater filtered through a 0.22 μm filter continuously mixed with a magnetic stirrer. Respiration was measured as oxygen uptake during the dark period. The dissolved

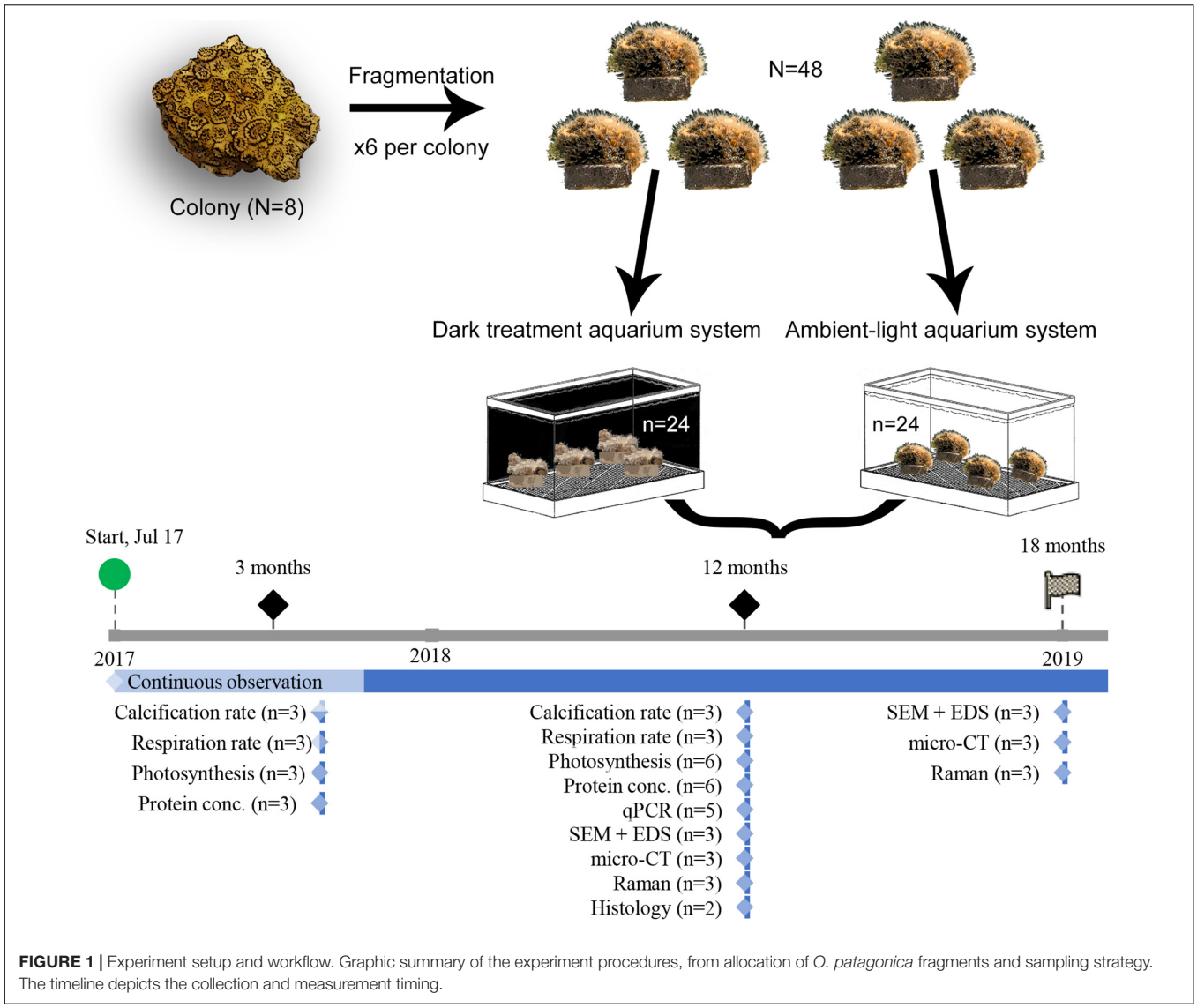

FIGURE 1 | Experiment setup and workflow. Graphic summary of the experiment procedures, from allocation of *O. patagonica* fragments and sampling strategy. The timeline depicts the collection and measurement timing.

oxygen concentration in the medium was measured for 1 h with an OX-N microsensor connected to a Microsensor Multimeter (Unisense, Denmark). The OX-N sensor was calibrated using a 2-points calibration; water saturated with dissolved oxygen following 5 min of vigorous bubbling with air (100%) as recommended by the user manual, whereas anoxic (0%) seawater was created by supersaturation with sulfide antioxidant buffer (cat 941609, Thermo-Fisher, United States). All measurements took place in complete darkness at a constant water temperature corresponding to the ambient temperature at the time of the measurement (3 months: 27°C, 12 months: 29°C and 18 months: 18°C). Dark respiration rates were normalized to the sample protein concentration, measured as described below.

Calcification Rates

Calcification rate was determined using the total alkalinity (TA) anomaly method with some modification (Chisholm and Gattuso, 1991). In brief, each fragment was sealed in a specimen cup filled with 0.22 μm of filtered artificial seawater and kept in their respective aquarium system for 5 h. Water samples were collected for TA at the beginning and the end of the incubation and were filtered again to remove debris and measured with an automatic alkalinity titrator (855 Robotic Titrosampler, Metrohm, Switzerland). The calcification rates [μmol $CaCO_3$ h^{-1} mg^{-1}] were then calculated using the equation proposed by Schneider and Erez (2006):

$$Calcification\ rate = \frac{\Delta TA * (V_{Chamber} - V_{Coral}) * 1.028}{T * P} \quad (1)$$

where ΔTA [μmol g^{-1}] is the difference in alkalinity between the beginning and the end of the incubation period; V is the recorded volume of the artificial seawater in the respective incubated cup [ml]; 1.028 is the density of seawater of the Eastern

Mediterranean [g ml^{-1}]; P is the measured total protein of the coral (mg); T is the duration of the incubation [hours].

Histology

The samples were fixed in 4% formaldehyde solution in seawater for 24 h. Decalcification was carried out using a solution of formic acid and sodium citrate for 24 h (Rinkevich and Loya, 1979). After decalcification, the tissue was rinsed in fresh water and transferred into 70% ethanol. Tissue was then embedded into paraffin blocks and 4 μm sections were obtained and stained with hematoxylin and eosin (Ventana BenchMark Fully Automated Slide Stainer System, Roche Diagnostics, Switzerland). Polyp sections were examined under a light microscope (Nikon Eclipse *Ti*, Japan).

Zooxanthellae Isolation, Protein and Pigment Study

After measuring respiration and calcification rates the same fragments were frozen in liquid nitrogen and kept in −80°C. Coral tissue was removed by an airbrush connected to a reservoir of phosphate buffer saline (PBS) solution filtered through a 0.22 μm filter, and the skeletons were kept for further analysis. The extracted tissue was mechanically disrupted using an electrical homogenizer (HOG-160-1/2, MRC-labs, Israel) for 3 × 10 s.

The homogenate was centrifuged at ×5000 g for 5 min at 4°C to separate the debris and the symbiont cells from the coral host tissue. A protease inhibitor cocktail (cat. G652A, Promega, United States) was added to the supernatant with the host tissue and sonicated for 3 × 30 s (Ultrasonic cell crusher, MRC-labs, Israel). The protein concentration of the coral host was determined using the fluorometric BCA protein kit (Pierce BCA, United States) following the manufacturer protocol. A PerkinElmer (2300 EnSpire®, United States) plate reader was used to determine the total protein concentration with a 540 nm wavelength emission.

The density of zooxanthellae in the homogenate was determined by fluorescent microscopic counts (Nikon Eclipse *Ti*, Japan*)* using a hemocytometer (BOECO, Germany) and 5 replicate (1 mm^2 each) cell counts per sample. Each replica was photographed both in brightfield and in fluorescent light using 440 nm emission to identify chlorophyll. Cell counting was performed using NIS-Elements Advanced Research (version 4.50.00, Nikon, Japan) with 0.5 < Circularity < 1, and the typical diameter parameter was to set between 5 and 15 μm.

Chlorophyll-*a* (chl-*a*) concentrations were measured in 2 ml of tissue homogenate that was filtered onto a Whatman GF/C filter and incubated overnight with 1 ml of 90% cold acetone at 4°C. After incubation, the filter was manually homogenized, and the solution was filtered into a glass cuvette through a 0.22 μm syringe filter. A NanoDrop (Thermo-Fisher, United States) was used for spectrophotometric measurements at wavelengths of 630, 647, 664 and 691 nm, and the light absorbance results were used to calculate the chl-*a* concentration based on the following equation (Eq. 2) (Ritchie, 2008).

$$Chl-a\ [\mu g\ ml^{-1}] = -0.3319 * ABS_{630} - 1.7485 * ABS_{647} + 11.9442 * ABS_{664} - 1.4306 * ABS_{697} \quad (2)$$

Skeleton Analysis

The soft tissue of Amb12/Dark12 and Amb18/Dark18 was removed by immersing the fragments in 1% sodium hypochlorite (NaClO) for 5 h. Thereafter, samples were rinsed with tap water filtered with a 0.22 μm filter followed by drying overnight at 45°C. The cleaned skeletons were imaged as follows.

Scanning Electron Microscopy (SEM) + Energy Dispersive X-Ray (EDS)

Samples were coated with gold prior to examination under a ZEISS Sigma™ SEM (Germany) coupled with EDS, by using an in-lens detector (5 kV, WD = 5–7 mm). Elemental analyses were performed in points of interest that were chosen after imaging in the SEM (20 kV, WD = 8 mm). Elemental distribution maps were obtained using AZtec (v2.2, Oxford Instruments, United Kingdom).

Micro Computed Tomography (CT)

Laboratory micro-CT (Skyscan 1275 and 1172, Bruker micro-CT, Belgium) instruments were used to image the specimens in 3D (9 μm pixel size, 360° scans, 60, 70 and 100 keV). Following reconstruction (NRecon 1.7, Bruker micro-CT, Belgium) the full architecture of the corals was examined in both 2D and 3D (ImageJ 1.52d, National Institutes of Health, United States; CTvox, Bruker micro-CT, Belgium).

Raman Spectroscopy

Raman measurements were conducted on a LabRAM HR Evolution instrument (Horiba, France) allowing for Raman spectra from 50 cm^{-1} and onward. The instrument is equipped with an 800 mm spectrograph which allows for sub wavenumber pixel spacing when working with 600 grooves/mm grating at 532 nm excitation. The sample was exposed to the laser light by an ×50 LWD NA 0.5 objective (LMPlanFL N, Olympus, Japan). The LabRAM instrument is equipped with a 1024 × 256 pixel open-electrode front illuminated with a cooled CCD camera. The system is set around an open confocal microscope (BX-FM Olympus, Japan) with a spatial resolution better than 2 μm using an ×50 objective. Exposure was set according to the signal intensity and exposures between 15 s and 1 min were used.

RNA Extraction, Transcriptome Assembly and Quantitative Real-Time PCR (qPCR)

RNA extraction was executed by using the PureLink® RNA Mini Kit (Cat. 12183025, Invitrogen, United States) following the manufacturer's protocol, with minor modifications. Briefly, each fragment was placed in liquid nitrogen until completely solidified and ground to a powder using a prechilled pestle and mortar. The

powder was transferred into a 2ml tube filled with 1.2 ml TRIzol reagent (Cat. 15596026, Invitrogen, United States) and incubated at room temperature for 15 min. Next, samples were transferred to QIAshredder tubes (Cat. 79656, Qiagen, Germany) and centrifuge for 3 min. The sample was then transferred to a new tube for phase separation with bromochloropropane (Cat. 109-70-6, Sigma). The RNA concentration and quality were evaluated using the NanoDrop 2000c (Thermo Scientific, United States) and the 2200 TapeStation (Agilent, United States). RNA integrity and quality cutoffs were of RNA integrity number (RIN) >8, the 260/280 nm ratio between 1.8 to 2.1 and 260/230 nm ratio ≥ 1.5. 500 ng of total RNA from each independent biological replicate was used to generate cDNA with the RevertAid First Strand cDNA Synthesis kit (cat. K1622, Thermo Scientific, United States) and RNA-seq libraries.

RNA of *O. patagonica* colonies that were collected in August 2016 was used to assemble *de novo* transcriptome. Sequencing libraries were prepared using the stranded Truseq mRNAseq protocol. 125 bp PE reads were sequenced on an Illumina HiSeq 2500v4 (3/4 lane).

Trinity pipeline (Freedman, 2016) was followed: Adapter sequences and low-quality bases were trimmed using cutadapt (Martin, 2011). Sequencing errors were corrected using Rcorrector (Song and Florea, 2015), and all reads that were not correctable were discarded. Reads were aligned to the genomes of the following known contaminants: *phiX* (Illumina igenome), *Symbiodinium kawagutii* (Lin et al., 2015), *Symbiodinium minutum* (Shoguchi et al., 2013), *Symbiodinium aenigmaticum, Symbiodinium pseudominutum, Symbiodinium psygmophilum* (Parkinson et al., 2016), and known rRNA sequences (Quast et al., 2012) using Bowtie2 (Langmead and Salzberg, 2012) with the setting –very-sensitive-local; reads with alignments were removed. Remaining reads were assembled into transcripts using Trinity (Grabherr et al., 2011) (v2.2.0). Assembly quality for each transcript was assessed using TransRate (Smith-Unna et al., 2016) (v1.0.3). Only transcripts with p_good >0 score were used for further analysis. A representative transcript with the highest p_good score was selected from each Trinity "gene." RSEM v.1.3.0 (Li and Dewey, 2011) was used for quantifying gene expression. Genes with <10 supporting reads were discarded.

Orthologs of the assembled transcripts were identified using BLASTX (NCBI) to align with the non-redundant (nr) protein database (downloaded on 17-Jul-2017). GO term annotation was added using Blast2GO (Conesa et al., 2005). Data availability and accession numbers Illumina short read sequences generated in this study have been submitted to the NCBI Sequence Read Archive (SRA)[1] under accession number PRJNA549836.

Based on *O. patagonica de novo* transcriptome, primers for qPCR were designed for genes representing different functions (**Table 1**) using Primer-Blast website (Ye et al., 2012). qPCR was

[1]http://www.ncbi.nlm.nih.gov/sra

TABLE 1 | Primers list for real-time qPCR.

Gene	Abbreviation	Primer ID	Primer sequence (5' → 3')	Amplicon size (bp)	Gene ontology term function
Actin	Actin	242090_c2_g6_i2_A_F	5′-CGGAATCGTTACCAACTGGGA-3′	192	Normalizing gene
		42090_c2_g6_i2_A_R	5′-TGGATAGCAACGTACATAGCAGG-3′		
Heat shock protein 70	HSP70	250834_c1_g1_i5_B_F	5′-ACCATCACCAACGACAAGGG-3′	173	Stress response
		250834_c1_g1_i5_B_R	5′-TCAACGTTTGGATCTTCTACCG-3′		
Complement C3	C3	239365_c0_g1_i6_A_F	5′-CCATGACGGCTTTTGTGTTA-3'	210	Innate immunity
		239365_c0_g1_i6_A_R	5′-TAGCGCTTTGCACAAGTCGG-3′		
Caspase 3	Cas3	245153_c1_g2_i5_B_F	5′-TGAGGAAGGTTTGGTGTATGG-3′	138	Cell apoptosis
		245153_c1_g2_i5_B_R	5′-TCCATGAACTCTGTGCCTTG-3'		
Carbonic anhydrase 2	CA2	247223_c0_g2_i7_A_F	5'-ACCTCATGCCCTACAACAATAA-3′	103	Calcification
		247223_c0_g2_i7_A_R	5′-TCCTCATCTCCACTACCATCA-3′		
Coral Acid Rich Protein 1	CARP1	250751_c0_g1_i1_B_F	5′-GAGATGAGAAGCTGGCTGTT-3′	98	Calcification
		250751_c0_g1_i1_B_R	5′-GTTAGTTTGCCGTCCTTGTTG-3'		
Mitochondrial-processing peptidase subunit beta	PMPCB	254524_c0_g1_i3_A_F	5′-AGACACTGGACTCTGGGGTA-3′	203	Aerobic respiration
		254524_c0_g1_i3_A_R	5′-TTTGTCGTCCGATGTCCTCA-3′		
Mitochondrial fission regulator 2	MTFR2	251372_c0_g1_i1_A_F	5′-CCTCAATCATCGCACAAG-3′	75	Aerobic respiration
		251372_c0_g1_i1_A_R	5′-TGGCATCTGGAGAGTTAG-3′		
NADH dehydrogenase flavoprotein 1	NDUFV1	255909_c3_g2_i5_A_F	5′-AGTTATTGGTGGCTGGGACA-3′	183	Aerobic respiration
		255909_c3_g2_i5_A_R	5′-ATGGCAAGGATGAGGTCACA-3′		
Chymotrypsinogen	CTR	241172_c0_g2_i1_C_F	5′-TATGTACGGCAACACAATGG-3′	106	Digestion
		241172_c0_g2_i1_C_R	5′-GTCAACCTTTGCTAGTGTCC-3′		

Designed based on O. patagonica's transcriptome.

performed on 5 samples from the Amb12 and Dark12 groups, using Fast SYBR Green Master Mix (cat. 4385612, Applied biosystems, United States) according to the manufacturer's instructions, and using a StepOnePlus® Real-Time PCR system (Applied Biosystems, United States). Each experiment was normalized with the actin gene using the comparative C_T method (Schmittgen and Livak, 2008).

Statistical Analysis

All the data was examined for homogeneity of normality (Shapiro-Wilk test) and equality of error variances (Levene's test). For qPCR relative quantification, an independent sample *t*-test was performed. For all other measurements, One-Way ANOVA was used ($P < 0.05$), followed by Bonferroni correction for *post hoc* comparisons, in which significant groups have a value of $P < 0.05$. Results are presented as mean ± standard error throughout. All statistical analyses were performed using IBM SPSS statistics (v20, United States).

RESULTS

Loss of pigmentation was noticeable for the *O. patagonica* fragments in the dark environment, primarily in the coenosarc and later in the corallite (**Figure 2** and **Supplementary Figures 1, 2**). Moreover, less than 1% of the zooxanthellae population was retained in the dark environment, in comparison to the ambient-light environment (**Figure 3A** and **Table 2**) (One-Way ANOVA, $F_{3,8} = 848.512$, $P < 0.001$).

However, the chl-*a* concentration per zooxanthella was significantly increased by two orders of magnitude in the Dark12 group (One-Way ANOVA, $F_{3,8} = 161.566$, $P < 0.001$) (**Figure 3B** and **Table 2**).

Photosynthetic efficiency was 50% lower in Dark3 compare to all other samples (One-Way ANOVA, $F_{3,8} = 34.739$, $P < 0.001$) (**Figure 3C** and **Table 2**).

Dark Respiration and Calcification Rates

Dark respiration rates (**Figure 4A** and **Table 2**) of Dark3, showed the highest rate was ∼127% higher than the rates at the parallel time point of the Amb3 group. On the contrary, the Dark12 group presented the lowest rate of dark respiration, compared to all other samples, and presented the highest rates of respiration which was approximately 73% lower than that of Amb12 (One-Way ANOVA, $F_{3,8} = 2.383$, $P < 0.001$).

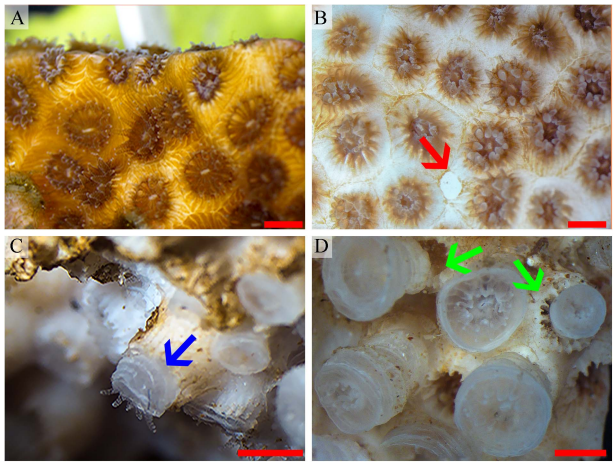

FIGURE 2 | *O. patagonica* macromorphology. *O. patagonica* images representing the bleaching process and the skeletal macromorphology transformation throughout the time of the experiment. Day 1, fully pigmented colony **(A)**, day 30, loss of the colony pigmentation and degradation of the coenosarc (red arrow) **(B)**, day 350 **(C)** and day 500 **(D)**. Blue arrow points to region of growth of the theca and green arrows highlight differences in the overlap of the newly formed thecae as compared with the shape formed in the ambient condition. Scale bar = 2 mm.

Dark3 group is exhibiting the lowest (and negative) rates of calcification compared to all other samples (**Figure 4B** and **Table 2**). However, Amb3, Amb12 and Dark12 did not show a significant difference between samples with calcification rates ranging between 0.113 and 0.15 μmol $CaCO_3$ hr^{-1} mg^{-1} protein (one-way ANOVA, $F_{3,8} = 12.379$, $P = 0.002$).

Changes in Coral Morphology

The transformation from colonial life to a solitary one was observed in the dark environment with the degradation of the connective tissue (coenosarc) (**Figures 2**, **5**, **6**, and **Supplementary Figure 1**), yet gametes were detected in both study environments (**Supplementary Figure 2**). Observation of a new skeleton wall (theca) formation is only noticeable at the corallite and not in the areas between the different polyps, resulting in a vertical extension of the corallite (**Figure 2C**; blue arrow, **Figure 6**; blue arrows). The newly formed theca in the dark, does not necessarily continue to form as an extension of the old one but can form as an internal and external structure of the corallite, though overlapping in certain areas of the original theca

TABLE 2 | Values of zooxanthellae cell count, chl-*a* concentration, photosynthesis efficiency, hourly respiration rate and hourly calcification rate per protein (±SE) in the different study time points and environments ($n = 3$ per time point and environment).

Group	Zooxanthellae count [cells mg^{-1}]	Chlorophyll-*a* [μg zooxanthella^{-1}]	Photosynthesis efficiency [Fv/Fm]	Respiration rate [μmol O_2 h^{-1} mg^{-1}]	Calcification rate [μmol $CaCO_3$ h^{-1} mg^{-1}]
Amb3	$2.92 \times 10^6 \pm 4.97 \times 10^4$	$1.87 \times 10^{-5} \pm 8.82 \times 10^{-7}$	0.473 ± 0.011	0.148 ± 0.017	0.15 ± 0.015
Dark3	$2.53 \times 10^4 \pm 1.38 \times 10^4$	$8.7 \times 10^{-5} \pm 6.51 \times 10^{-6}$	0.217 ± 0.035	0.336 ± 0.03	−0.036 ± 0.012
Amb12	$3 \times 10^6 \pm 1.05 \times 10^5$	$9.63 \times 10^{-6} \pm 3.29^{*}10^{-6}$	0.538 ± 0.013	0.19 ± 0.018	0.113 ± 0.023
Dark12	$1.82 \times 103 \pm 4.45 \times 10^2$	$1.08 \times 10^{-3} \pm 8.2 \times 10^{-5}$	0.463 ± 0.028	0.051 ± 0.015	0.125 ± 0.038

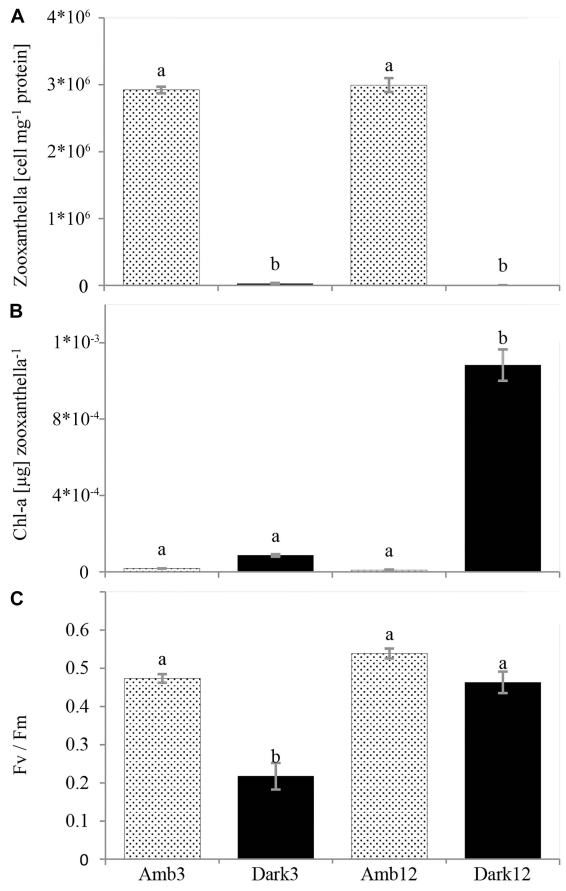

FIGURE 3 | *O. patagonica* mean photosynthetic parameters (±SE, *N* = 3, per timepoint). Zooxanthellae count per host protein **(A)**, chlorophyll-*a* concentration per zooxanthella **(B)**, and Fv/Fm **(C)**. Different lowercase letters indicate significantly different samples (see **Table 2** for exact values).

(**Figure 2D**; green arrows, **Figure 5**, **Supplementary Figures 4, 5**, and **Supplementary Video 1**). The dark environment thecae are less dense and have a smoother surface (**Figure 5**; red arrows). While septa formation appears to become halted in the dark environment groups, newly formed spines demonstrate a similar appearance to the costas (the extension of the septa outside the upper surface of the corallite) in the ambient-light colonies (**Figure 5F**; green arrows, **Supplementary Figure 4**, and **Supplementary Video 2**). Furthermore, internal spines are observed where septa are expected (**Figure 6**; yellow arrows and **Supplementary Videos 1, 2**). Elemental composition, as shown by EDS (**Supplementary Figure 6**), indicates that the skeletons formed in both sample groups consist of Ca^{2+}, while the Raman spectra (**Figure 7**) clearly prove that the new skeleton structures are made from aragonite. This $CaCO_3$ polymorph is characterized by the peaks at 152.4 (B1g), 205 (B2g), 702.6 (B3g), 705.6 (Ag) and 1085.6 (Ag) cm^{-1} (Frech et al., 1980; De La Pierre et al., 2014).

Gene Expression

While gene expression in the Dark12 measurements regarding stress response (*HSP70*), innate immunity (*C3*), apoptosis (*Cas3*) and calcification (*CA2* and *CARP1*) are significantly lower as compared to the Amb12 measurements (**Figure 8**). The chymotrypsinogen gene (*CTR*), that takes part in the digestion process did not show any significant change in expression. Whereas two out of the three genes related to aerobic respiration process – *MTFR2* and *NDUFV1* – were significantly overexpressed for Dark12, *PMPCB* was not differentially expressed in the various samples.

DISCUSSION

The vulnerability of zooxanthellate stony corals to changing climate is well documented, resulting in bleaching and mortality (Hughes, 2003; Hughes et al., 2018; van Oppen and Lough, 2018). Yet, not all species are affected at the same intensity and some are able to survive and thrive.

In this study, we suggest that the temperate stony coral, *Oculina patagonica* is able to survive and possibly thrive without the assistance of their photosynthesizing endosymbionts by

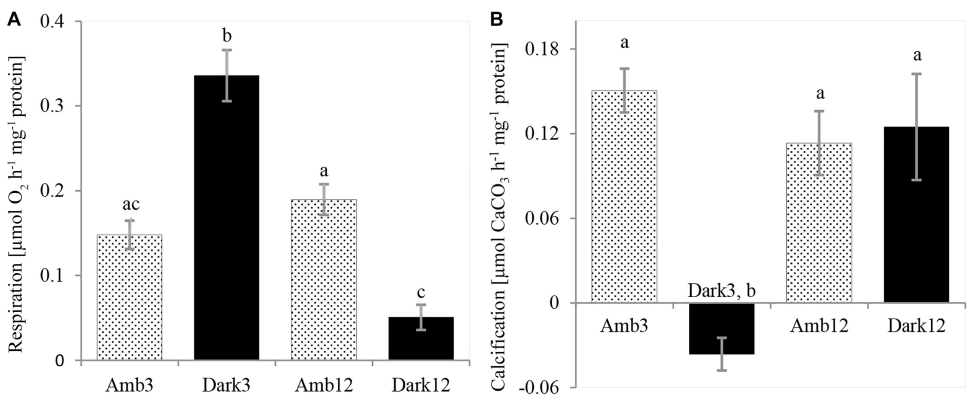

FIGURE 4 | *O. patagonica* physiology rates. *O. patagonica* Mean (±SE) dark respiration rate **(A)** and calcification rate **(B)** of the different samples (*N* = 3 per timepoint). Different lowercase letters indicate significantly different samples (see **Table 2** for exact values).

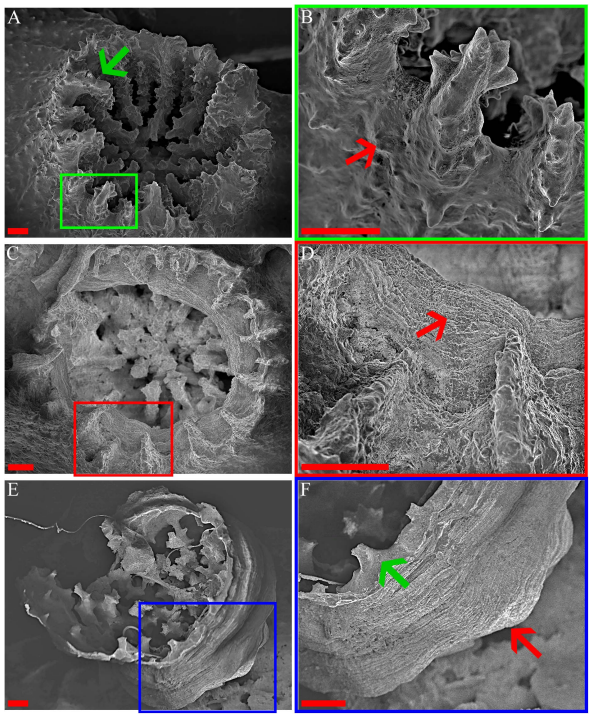

FIGURE 5 | *O. patagonica*'s micromorphology. SEM images showing *O. patagonica* micromorphology for ambient-light **(A,B)** and the dark samples at the 12 **(C,D)** and 18 **(E,F)** time points. Green, red and blue regions indicate higher-magnification insets. The red arrows point to the coarser thecae and septa of the ambient-light samples compared to the smoother thecae of the dark samples **(B,D,F)**. Note (green arrow) the start of a costa formation in the Dark compared to the ambient-light **(A,F)**. Scale bar = 200 μm.

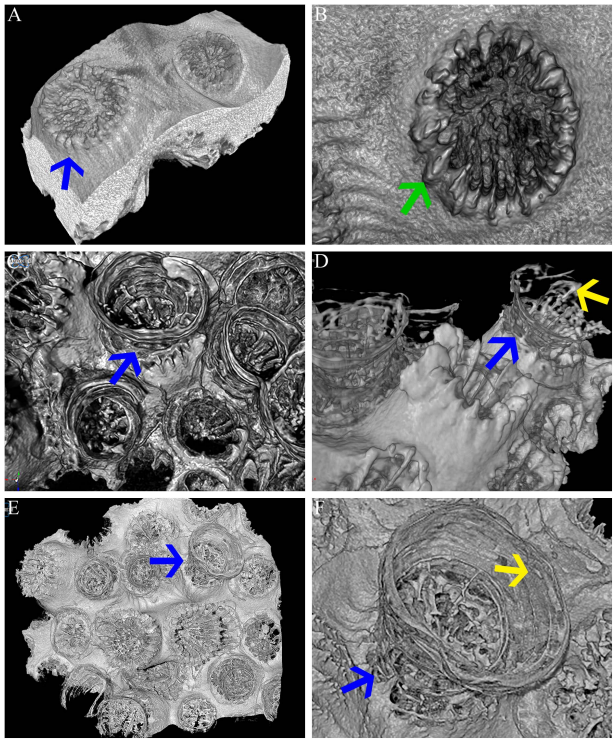

FIGURE 6 | Micro-CT. Micro-CT images showing *O. patagonica* micromorphology for ambient-light **(A,B)** and the dark samples at the 12 **(C,D)** and 18 **(E,F)** time points. Blue arrows identify the continuous vertical growth of the corallites in the dark samples **(A,C–F)**. Yellow arrows point to recurring internal bulges observed in the dark treated colonies **(D,F)**. Green arrow indicates regular costa formation in the ambient-light samples **(B)**.

modulating its physiology, morphology and gene expression pattern. We observe a two-stage mechanism: (i) acclimation of the coral host to a bleached state by increasing its metabolic rate and reducing non-essential functions, such as calcification and (ii) adaptation by decreasing their metabolic rate and regaining the ability to invest energy in non-essential functions.

As a result of the translocation of the coral colonies to the dark, the symbiosis between the coral host and the symbiotic algae (zooxanthellae) breaks down (**Figure 3A** and **Table 2**), depriving energy of the coral host, which until then was supplied by the algae. This is then followed by lower calcification rates (**Figure 4B** and **Table 2**), tissue degradation and a transition from colonial life to a solitary one (**Figure 2** and **Supplementary Figures 1, 2**). Fragments visually lost their pigmentation after 20 days (**Figure 2**), a timeframe similar to other reports in temperate corals (Kevin and Hudson, 1979). However, at Dark12, zooxanthellae cell counts revealed traces of the zooxanthellae population with higher chl-*a* concentration per alga (**Figures 3A,B** and **Table 2**) and the photosynthesis efficiency of the bleached colonies was statistically similar to the ambient-light samples (**Figure 3C** and **Table 2**). These results are in agreement with previous reports of photoadaptation for corals in low light or light-limited corals (Falkowski and Dubinsky, 1981; Titlyanov et al., 2001; Stambler and Dubinsky, 2004; Cohen and Dubinsky, 2015). Interestingly, previous studies of the zooxanthellae population dynamics during repeated seasonal bleaching on *S. pistillata* (Nir et al., 2014) showed an opposite trend where *S. pistillata* zooxanthellae population did not change but the Chl-*a* per alga declined. Nevertheless, seasonal bleaching, as its name implies, is only temporary and may not leave enough time for the most robust zooxanthellae population to adapt to its changing environment. Indeed, a long-term study on the depth-dependent photoacclimation of *S. pistillata* showed that the chlorophyll concentration per algal cell is only increasing after 6 months (Cohen and Dubinsky, 2015).

During the first stage, where the coral host needs to overcome the lack of energy, the rate of respiration increases (**Figure 4A** and **Table 2**), which can increase ATP supply by oxidative phosphorylation (Edmunds et al., 2011; Schrameyer et al., 2014; Cohen et al., 2016; Galli and Solidoro, 2018). While the exact mechanism of bleaching is unknown and it might involve multiple cellular processes (Tolleter et al., 2013; Oakley and Davy, 2018), it is primarily considered as a result of the accumulation of toxic reactive oxygen species (ROS) (Downs et al., 2002). Although increased light intensity is the main reason for the formation of harmful ROS, previous studies have reported the formation of ROS in the dark as well as a result of photodamage to the zooxanthellae chloroplast,

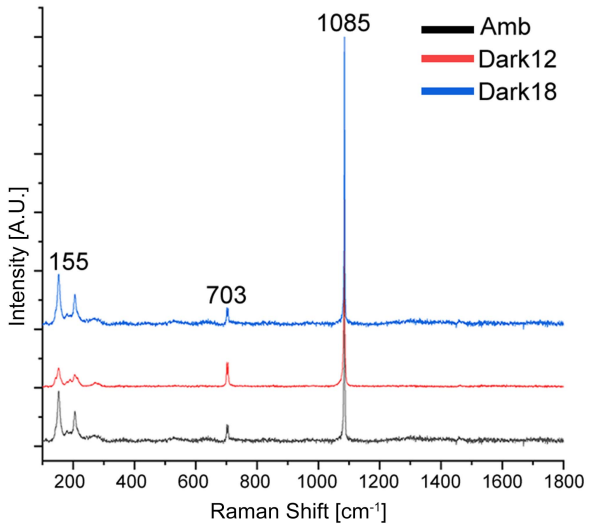

FIGURE 7 | Raman measurements of aragonite minerals in *O. patagonica* corallites. Average spectra for colonies grown under ambient (black) and bleaching conditions, measured after 12 (red) and 18 (blue) months. Samples spectra correspond to aragonite, with the known peaks overlapping at ~155–280, ~703 and ~1085 cm^{-1}.

similar to plants (Choudhury and Biswal, 1979; Saragosti et al., 2010; DeSalvo et al., 2012; Zhang et al., 2016). We propose that the increased respiration rate of the coral host helps in decreasing ROS production (Barros et al., 2004). The excess ROS produced by the algae, and possibly by the coral host as well, have been suggested to activate a caspase cascade within the host cell, which in turn can result in tissue apoptosis and eventually lead to the death of the host (Tchernov et al., 2011). In our experiment, *O. patagonica* tissue degradation is noticeable after the loss of the endosymbiont algae, predominantly in the host coenosarc (**Figure 2** and **Supplementary Figure 1**). The disappearance of the coenosarc leads to *O. patagonica* transitioning from colonial life to a solitary one, in which each polyp needs to sustain itself. A similar transformation can be found in nature within the Red Sea coral, *Lobophyllia corymbosa*, where it was proposed to result in better protection from pathogens (Brickner et al., 2006). The transformation to a solitary life was previously recorded for *O. patagonica* in separate low pH treatment and cold thermal stress studies (Fine and Tchernov, 2007; Serrano et al., 2017). This transformation also led to a strong reduction in calcification activities, which resumed only after restoration to a colonial life. However, to the best of our knowledge, this is the first time that such a transformation has been shown in dark-treated corals.

As a continuation of the acclimation stage, *O. patagonica* shows no evidence of calcification (**Figure 4B** and **Table 2**). Our results of a negative calcification rate cannot be attributed to decalcification since careful attention was paid to ensure that normal pH values were maintained in our closed study systems. However, it has been previously established that at night, coral tissue does decrease the surrounding pH as compared to the values in the sea water, presumably because the endosymbiont algae do not fix CO_2 at night (Kühl et al., 1995). Thus, it is possible that some decalcification occurs in the dark acclimated corals, similarly to previous reports for *O. patagonica* under pH stress, albeit at reduced capacity (Fine and Tchernov, 2007).

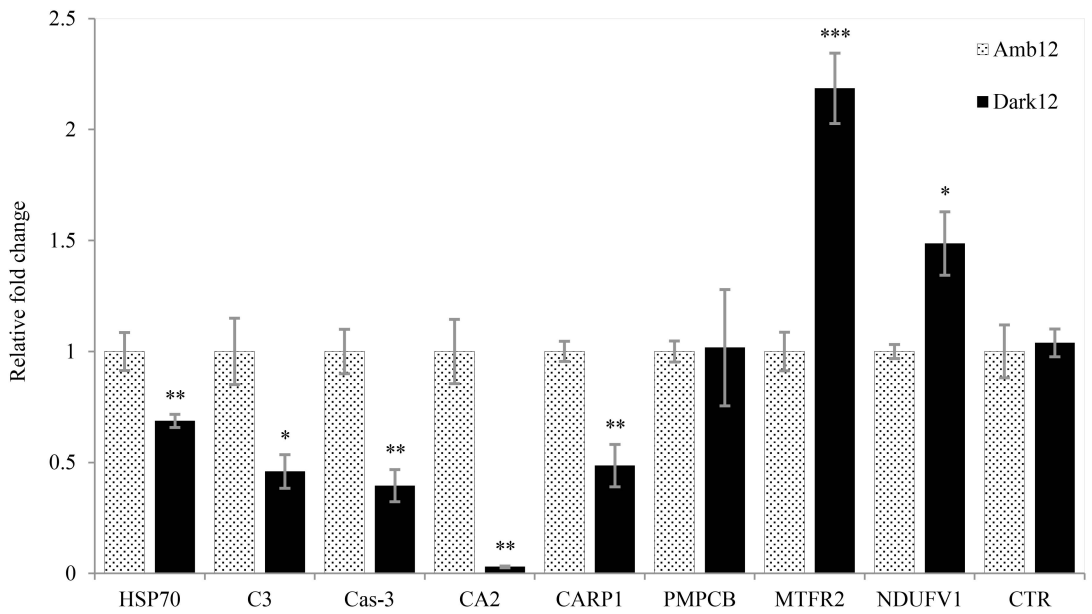

FIGURE 8 | Relative fold change of real-time qPCR. Mean (±SE) Gene expression results for the dark (Black bars) and ambient-light (light bars) samples at the 12-month time point using the gene comparative C_T method. The relative fold change was calculated based on the ambient-light samples data. Independent sample *t*-test. *$p < 0.05$; **$p < 0.01$; ***$p < 0.001$ ($N = 5$).

In the second stage, *O. patagonica* fragments show continuous gametogenesis (**Supplementary Figure 3**), appear to lower their metabolic rate and resume calcification activity (**Figure 4** and **Table 2**). The gene expression patterns (**Figure 8**) show that two of the aerobic respiration-related genes are overexpressed (*MTFR2*, and *NDUFV1*). This may imply that the bleached *O. patagonica* is continuing to reallocate its limited resources toward energy production and survival, as it did during the first stage of acclimation. As previously mentioned, activation of a caspase cascade can result in the degradation, by apoptosis, of the coenosarc, a process that matches the profiles of caspase-3 activity and gene expression (Kvitt et al., 2011). Here we found that caspase-3 is downregulated in the Dark12 compared to Amb12 (**Figure 8**), further suggesting of a recovery stage by the coral (Tchernov et al., 2011). The expression of *HSP70* (**Figure 8**) further supports the coral's adaptation to the dark environment. *HSP70* is a well establish stress-induced gene (Maor-Landaw et al., 2014). The underexpression of *HSP70* in the bleached *O. patagonica* is similar to their representative expression in Mediterranean azooxanthellate corals compare to zooxanthellate corals (Franzellitti et al., 2018). However, underexpression of *HSP70* may cause future difficulties to the coral if other stressors appear, such as a thermo-shock due to an extensive increase in seawater temperature (Gong, 2005). Gene expression of complementary C3 (**Figure 8**), which is part of the innate immune pathways that are involved in the ability of the coral to differentiate between pathogens and mutual symbiosis (McFall-Ngai, 2007; Eberl, 2010; Poole et al., 2016) is also underexpressed. This raises concern regarding the ability of the bleached *O. patagonica* to endure multiple stressors and diseases.

It is considered that one of the methods used by corals to survive bleaching events is to increase their heterotrophic feeding rates (Grottoli et al., 2006; Hoogenboom et al., 2010). This method was also suggested as a strategy for *O. patagonica* to survive during repeated bleaching events (Armoza-Zvuloni et al., 2011). Chymotrypsinogen is an important digestive enzyme found in organisms from every taxonomic group in the evolutionary tree and was recently isolated in the tropical coral *Stylophora pistillata* (Raz-Bahat et al., 2017). Although there was no difference in expression between samples (**Figure 8**), the fact that this gene is not downregulated in the bleached colonies hints to the importance of maintaining the enzyme's availability so that when food is present, this enzyme is available to the coral.

As previously noted, the coral fragments had arrested their calcification activity, which can be related to the transformation to a solitary life, similarly to Serrano et al. (2017) study, which we propose is part of the acclimation stage as it is for only a short period. However, here we demonstrate that solitary bleached *O. patagonica* polyps do restore their calcification activity (**Figure 4B** and **Table 2**), which is related to the adaptation stage. However, it is noticeable that the newly formed skeleton has a different morphology. The newly formed skeleton bulges out (**Figures 2C,D**, **5D,F**, **6C–F** and **Supplementary Videos 1, 2**), the thecae (corallite wall) are markedly less dense and they are lacking septa (**Figures 5C,D**, **6** and **Supplementary Video 2**) compared to the ambient-light samples. In addition, distinct calcification related genes (*CA2* and *CARP1*) are underexpressed (**Figure 8**). Those changes might depict an environmental-induced variability of skeletal morphology, a phenotypic plasticity that aids the organisms in adjusting to different environments (Kaandorp, 1999; Kaandorp and Leiva, 2004; Mass and Genin, 2008; Ow and Todd, 2010; Tambutté et al., 2015). Although plasticity may not be the best strategy for short periods of environmental fluctuations, it is preferable for adapting to long term changes (Todd, 2008). Morphological plasticity can be found as a result of changing environmental factors such as light (Mass et al., 2007; Lesser et al., 2010) pH (Tambutté et al., 2015) and water flow (Kaandorp et al., 1996; Mass and Genin, 2008). Specifically, when light intensity diminishes, corals typically metamorphose to more of a planer morphology, resulting in the need to support less tissue (Stambler and Dubinsky, 2005). In *O. patagonica*, as long as the coenosarc was present and intact, the coral did not demonstrate any morphological changes (**Figures 2A,B**). However, once the calcification process by the organism resumed, the morphology of the coral changed from a plocoid colony structure to a phaceloid-like structure (**Figures 2C,D**), as each polyp secreted an aragonite (**Figure 7**) skeleton vertically (**Figures 2**, **5**, **6**). However, due to sample topography, the concentration of the elements cannot be calculated using this setup (Mor Khalifa et al., 2018). while the newly formed skeleton appear to be more delicate and might be easily damaged in case of a more turbulent environment (Chamberlain, 1978; Reyes-Nivia et al., 2013), there is evidence of septa and costa-like structures, especially at Dark18 (**Figures 5**, **6** and **Supplementary Video 1**), suggesting the coral is beginning to allocate resources toward structure support and not only for vertical growth. The reasons for prioritizing continuous vertical growth is unknown, however, it has been previously proposed that such a strategy might be advantageous for sessile organisms which compete for space and food (Chadwick and Morrow, 2011). Alternatively, it is possible that some unknown mechanism drives searching for light in higher places, a reasonable assumption in dark waters.

The data presented in this study further indicate that *O. patagonica* is a highly resilient scleractinian species and is able to discard potentially damaging and energetically costly elements. As not all coral species are affected similarly to the changing environment, where some appear to be more resilient "winners" than other "losers" (Fabricius et al., 2011; Hubbard and Dullo, 2016), better understanding of the mechanisms that allow *O. patagonica* to adapt and succeed, following bleaching might prove valuable in studying the biological system and pathways involved in enhancing tolerance for corals to environmental stress (van Oppen et al., 2017; Cornwall, 2019).

DATA AVAILABILITY STATEMENT

The datasets generated for this study can be found in the NCBI Sequence Read Archive under accession number PRJNA549836.

AUTHOR CONTRIBUTIONS

TZ collected and analyzed the data with support from TM in planning and reporting. TM and TZ wrote the manuscript.

PZ contributed the micro-CT data. IP contributed the micro-Raman data. All authors contributed to the writing and improving of the manuscript and approved its final version.

FUNDING

This research was supported by the United States–Israel Binational Science Foundation Grant BSF-2016321.

ACKNOWLEDGMENTS

We thank Dr. E. Shemesh, Dr. R. Almuly, H. Nativ, and the technical staff of the Moris Kahn Marine Research Station for their invaluable help. We also thank The Mantoux Bioinformatics Institute of the Nancy and Stephen Grand Israel National Center for Personalized Medicine, Weizmann Institute of Science. This study was performed in accordance with regulations and guidelines set by the Israel Nature and Parks Authority.

SUPPLEMENTARY MATERIAL

The Supplementary Material for this article can be found online at: https://www.frontiersin.org/articles/10.3389/fmars.2019.00662/full#supplementary-material

REFERENCES

Armoza-Zvuloni, R., Segal, R., Kramarsky-Winter, E., and Loya, Y. (2011). Repeated bleaching events may result in high tolerance and notable gametogenesis in stony corals: oculina patagonica as a model. *Mar. Ecol. Prog. Ser.* 426, 149–159. doi: 10.3354/meps09018

Baker, A. C., Glynn, P. W., and Riegl, B. (2008). Climate change and coral reef bleaching: an ecological assessment of long-term impacts, recovery trends and future outlook. *Estuar. Coast. Shelf Sci.* 80, 435–471. doi: 10.1016/j.ecss.2008.09.003

Barros, M. H., Bandy, B., Tahara, E. B., and Kowaltowski, A. J. (2004). Higher respiratory activity decreases mitochondrial reactive oxygen release and increases life span in *Saccharomyces cerevisiae*. *J. Biol. Chem.* 279, 49883–49888. doi: 10.1074/jbc.M408918200

Berkelmans, R. (2018). "Bleaching and mortality thresholds: how much is too much?," in *Coral Bleaching*, eds M. J. H. van Oppen and J. M. Lough (Berlin: Springer), 213–230. doi: 10.1007/978-3-319-75393-5-9

Bessell-Browne, P., Negri, A. P., Fisher, R., Clode, P. L., Duckworth, A., and Jones, R. (2017). Impacts of turbidity on corals: the relative importance of light limitation and suspended sediments. *Mar. Pollut. Bull.* 117, 161–170. doi: 10.1016/j.marpolbul.2017.01.050

Brickner, I., Oren, U., Frank, U., and Loya, Y. (2006). Energy integration between the solitary polyps of the clonal coral *Lobophyllia corymbosa*. *J. Exp. Biol.* 209, 1690–1695. doi: 10.1242/jeb.02168

Chadwick, N. E., and Morrow, K. M. (2011). "Competition among sessile organisms on coral reefs," in *Coral Reefs: An Ecosystem in Transition*, eds Z. Dubinsky and N. Stambler (Dordrecht: Springer), 347–371. doi: 10.1007/978-94-007-0114-4-20

Chamberlain, J. A. (1978). Mechanical properties of coral skeleton: compressive strength and its adaptive significance. *Paleobiology* 4, 419–435. doi: 10.1017/S0094837300006163

Chisholm, J. R. M., and Gattuso, J. (1991). Validation of the alkalinity anomaly technique for investigating calcification of photosynthesis in coral reef communities. *Limnol. Oceanogr.* 36, 1232–1239. doi: 10.4319/lo.1991.36.6.1232

Choudhury, N. K., and Biswal, U. C. (1979). Changes in photoelectron transport of chloroplasts isolated from dark stressed leaves of maize seedlings. *Experientia* 35, 1036–1037. doi: 10.1007/BF01949926

Cohen, I., and Dubinsky, Z. (2015). Long term photoacclimation responses of the coral *Stylophora pistillata* to reciprocal deep to shallow transplantation: photosynthesis and calcification. *Front. Mar. Sci.* 2:45. doi: 10.3389/fmars.2015.00045

Cohen, I., Dubinsky, Z., and Erez, J. (2016). Light enhanced calcification in hermatypic corals: new insights from light spectral responses. *Front. Mar. Sci.* 2:122. doi: 10.3389/fmars.2015.00122

Conesa, A., Gotz, S., Garcia-Gomez, J. M., Terol, J., Talon, M., and Robles, M. (2005). Blast2GO: a universal tool for annotation, visualization and analysis in functional genomics research. *Bioinformatics* 21, 3674–3676. doi: 10.1093/bioinformatics/bti610

Cornwall, W. (2019). The reef builders. *Science* 363, 1264–1269. doi: 10.1126/science.363.6433.1264

Davies, S. P. (1984). The role of zooxanthellae in the nutritional energy requirements of pocillopora eydouxi. *Coral Reefs* 2, 181–186. doi: 10.1007/bf00263571

De La Pierre, M., Carteret, C., Maschio, L., André, E., Orlando, R., and Dovesi, R. (2014). The raman spectrum of CaCO3 polymorphs calcite and aragonite: a combined experimental and computational study. *J. Chem. Phys.* 140:164509. doi: 10.1063/1.4871900

DeSalvo, M. K., Estrada, A., Sunagawa, S., and Medina, M. (2012). Transcriptomic responses to darkness stress point to common coral bleaching mechanisms. *Coral Reefs* 31, 215–228. doi: 10.1007/s00338-011-0833-834

Donner, S. D., Heron, S. F., and Skirving, W. J. (2018). "Future scenarios: a review of modelling efforts to predict the future of coral reefs in an era of climate change," in *Coral Bleaching*, eds M. J. H. van Oppen and J. M. Lough (Cham: Springer), 325–341. doi: 10.1007/978-3-319-75393-5-13

Downs, C. A., Fauth, J. E., Halas, J. C., Dustan, P., Bemiss, J., and Woodley, C. M. (2002). Oxidative stress and seasonal coral bleaching. *Free Radic. Biol. Med.* 33, 533–543. doi: 10.1016/S0891-5849(02)00907-3

Dubinsky, Z., and Stambler, N. (eds) (2011). *Coral Reefs: An Ecosystem in Transition*. Dordrecht: Springer.

Eberl, G. (2010). A new vision of immunity: homeostasis of the superorganism. *Mucosal Immunol.* 3, 450–460. doi: 10.1038/mi.2010.20

Edmunds, P. J., Cumbo, V., and Fan, T.-Y. (2011). Effects of temperature on the respiration of brooded larvae from tropical reef corals. *J. Exp. Biol.* 214, 2783–2790. doi: 10.1242/jeb.055343

Fabricius, K. E., Langdon, C., Uthicke, S., Humphrey, C., Noonan, S., De'ath, G., et al. (2011). Losers and winners in coral reefs acclimatized to elevated carbon dioxide concentrations. *Nat. Clim. Chang.* 1, 165–169. doi: 10.1038/nclimate1122

Falkowski, P. G., and Dubinsky, Z. (1981). Light-shade adaptation of *Stylophora pistillata*, a hermatypic coral from the Gulf of Eilat. *Nature* 289, 172–174. doi: 10.1038/289172a0

Falkowski, P. G., Dubinsky, Z., Muscatine, L., and Porter, J. W. (1984). Light and the bioenergetics of a symbiotic coral. *Bioscience* 34, 705–709. doi: 10.2307/1309663

Fine, M., and Tchernov, D. (2007). Scleractinian coral species survive and recover from decalcification. *Science* 315:1811. doi: 10.1126/science.1137094

Fine, M., Zibrowius, H., and Loya, Y. (2001). Oculina patagonica: a non-lessepsian scleractinian coral invading the Mediterranean Sea. *Mar. Biol.* 138, 1195–1203. doi: 10.1007/s002270100539

Franzellitti, S., Airi, V., Calbucci, D., Caroselli, E., Prada, F., Voolstra, C. R., et al. (2018). Transcriptional response of the heat shock gene hsp70 aligns with differences in stress susceptibility of shallow-water corals from the mediterranean Sea. *Mar. Environ. Res.* 140, 444–454. doi: 10.1016/j.marenvres.2018.07.006

Frech, R., Wang, E. C., and Bates, J. B. (1980). The i.r. and Raman spectra of CaCO3 (aragonite). *Spectrochim. Acta Part A Mol. Spectrosc.* 36, 915–919. doi: 10.1016/0584-8539(80)80044-80044

Freedman, A. (2016). *Best Practices for De Novo Transcriptome Assembly with Trinity*. Available at: https://informatics.fas.harvard.edu/best-practices-for-de-novo-transcriptome-assembly-with-trinity.html (accessed July 17, 2017).

Frieler, K., Meinshausen, M., Golly, A., Mengel, M., Lebek, K., Donner, S. D., et al. (2013). Limiting global warming to 2°C is unlikely to save most coral reefs. *Nat. Clim. Chang.* 3, 165–170. doi: 10.1038/nclimate1674

Galli, G., and Solidoro, C. (2018). ATP supply may contribute to light-enhanced calcification in corals more than abiotic mechanisms. *Front. Mar. Sci.* 5:68. doi: 10.3389/fmars.2018.00068

Glynn, P. W. (1983). Extensive 'bleaching' and death of reef corals on the Pacific coast of Panama. *Environ. Conserv.* 10, 149–154.

Glynn, P. W. (1993). Coral reef bleaching: ecological perspectives. *Coral Reefs* 12, 1–17. doi: 10.1007/BF00303779

Gong, W. J. (2005). Loss of Hsp70 in drosophila is pleiotropic, with effects on thermotolerance, recovery from heat shock and neurodegeneration. *Genetics* 172, 275–286. doi: 10.1534/genetics.105.048793

Grabherr, M. G., Haas, B. J., Yassour, M., Levin, J. Z., Thompson, D. A., Amit, I., et al. (2011). Full-length transcriptome assembly from RNA-Seq data without a reference genome. *Nat. Biotechnol.* 29, 644–652. doi: 10.1038/nbt.1883

Graham, N. A. J., Jennings, S., MacNeil, M. A., Mouillot, D., and Wilson, S. K. (2015). Predicting climate-driven regime shifts versus rebound potential in coral reefs. *Nature* 518, 94–97. doi: 10.1038/nature14140

Grottoli, A. G., Rodrigues, L. J., and Palardy, J. E. (2006). Heterotrophic plasticity and resilience in bleached corals. *Nature* 440, 1186–1189. doi: 10.1038/nature04565

Grottoli, A. G., Warner, M. E., Levas, S. J., Aschaffenburg, M. D., Schoepf, V., McGinley, M., et al. (2014). The cumulative impact of annual coral bleaching can turn some coral species winners into losers. *Glob. Chang. Biol.* 20, 3823–3833. doi: 10.1111/gcb.12658

Høegh-Guldberg, O. (1999). Climate change, coral bleaching and the future of the world's coral reefs. *Mar. Freshw. Res.* 50:839. doi: 10.1071/MF99078

Hoogenboom, M., Rodolfo-Metalpa, R., and Ferrier-Pages, C. (2010). Co-variation between autotrophy and heterotrophy in the mediterranean coral cladocora caespitosa. *J. Exp. Biol.* 213, 2399–2409. doi: 10.1242/jeb.040147

Hubbard, D. K., and Dullo, W.-C. (2016). "The changing face of reef building," in *Coral Reefs at the Crossroads*, eds D. Hubbard, C. Rogers, J. Lipps, and G. Stanley (Dordrecht: Springer), 127–153. doi: 10.1007/978-94-017-7567-0-6

Hughes, T. P. (2003). Climate change, human impacts, and the resilience of coral reefs. *Science* 301, 929–933. doi: 10.1126/science.1085046

Hughes, T. P., Anderson, K. D., Connolly, S. R., Heron, S. F., Kerry, J. T., Lough, J. M., et al. (2018). Spatial and temporal patterns of mass bleaching of corals in the anthropocene. *Science* 359, 80–83. doi: 10.1126/science.aan8048

Hughes, T. P., Kerry, J. T., Baird, A. H., Connolly, S. R., Chase, T. J., Dietzel, A., et al. (2019). Global warming impairs stock–recruitment dynamics of corals. *Nature* 568, 387–390. doi: 10.1038/s41586-019-1081-y

Kaandorp, J. A. (1999). Morphological analysis of growth forms of branching marine sessile organisms along environmental gradients. *Mar. Biol.* 134, 295–306. doi: 10.1007/s002270050547

Kaandorp, J. A., and Leiva, R. A. G. (2004). "Morphological analysis of two- and three- dimensional images of branching sponges and corals," in *Morphometrics*, ed. A. M. T. Elewa (Berlin: Springer), 83–96. doi: 10.1007/978-3-662-08865-4-7

Kaandorp, J. A., Lowe, C. P., Frenkel, D., and Sloot, P. M. A. (1996). Effect of nutrient diffusion and flow on coral morphology. *Phys. Rev. Lett.* 77, 2328–2331. doi: 10.1103/PhysRevLett.77.2328

Kevin, K. M., and Hudson, R. C. L. (1979). The role of zooxanthellae in the hermatypic coral plesiastrea urvillei (milne edwards and haime) from cold waters. *J. Exp. Mar. Bio. Ecol.* 36, 157–170. doi: 10.1016/0022-09817990106-90100

Krom, M. D., and Suari, Y. (2015). The eastern mediterranean Sea. *Ocean Chall.* 21, 46–52.

Kühl, M., Cohen, Y., Dalsgaard, T., Jørgensen, B., and Revsbech, N. (1995). Microenvironment and photosynthesis of zooxanthellae in scleractinian corals studied with microsensors for O2, pH and light. *Mar. Ecol. Prog. Ser.* 117, 159–172. doi: 10.3354/meps117159

Kvitt, H., Rosenfeld, H., Zandbank, K., and Tchernov, D. (2011). Regulation of apoptotic pathways by *Stylophora pistillata* (Anthozoa, Pocilloporidae) to survive thermal stress and bleaching. *PLoS One* 6:e28665. doi: 10.1371/journal.pone.0028665

Langmead, B., and Salzberg, S. L. (2012). Fast gapped-read alignment with bowtie 2. *Nat. Methods* 9, 357–359. doi: 10.1038/nmeth.1923

Lesser, M. P., Slattery, M., Stat, M., Ojimi, M., Gates, R. D., and Grottoli, A. (2010). Photoacclimatization by the coral *Montastraea cavernosa* in the mesophotic zone: light, food, and genetics. *Ecology* 91, 990–1003. doi: 10.1890/09-0313.1

Li, B., and Dewey, C. N. (2011). RSEM: accurate transcript quantification from RNA-Seq data with or without a reference genome. *BMC Bioinformatics* 12:323. doi: 10.1186/1471-2105-12-323

Lin, S., Cheng, S., Song, B., Zhong, X., Lin, X., Li, W., et al. (2015). The *Symbiodinium kawagutii* genome illuminates dinoflagellate gene expression and coral symbiosis. *Science* 350, 691–694. doi: 10.1126/science.aad0408

Lough, J. M., and van Oppen, M. J. H. (2018). "Introduction: coral bleaching-patterns, processes, causes and consequences," in *Coral Bleaching: Patterns, Processes, Causes and Consequences*, eds M. J. H. van Oppen and J. M. Lough (Cham: Springer International Publishing), 1–8. doi: 10.1007/978-3-319-75393-5-1

Maor-Landaw, K., Karako-Lampert, S., Ben-Asher, H. W., Goffredo, S., Falini, G., Dubinsky, Z., et al. (2014). Gene expression profiles during short-term heat stress in the Red Sea coral *Stylophora pistillata*. *Glob. Chang. Biol.* 20, 3026–3035. doi: 10.1111/gcb.12592

Martin, M. (2011). Cutadapt removes adapter sequences from high-throughput sequencing reads. *EMBnet J.* 17, 10–12. doi: 10.14806/ej.17.1.200

Mass, T., Einbinder, S., Brokovich, E., Shashar, N., Vago, R., Erez, J., et al. (2007). Photoacclimation of *Stylophora pistillata* to light extremes: metabolism and calcification. *Mar. Ecol. Prog. Ser.* 334, 93–102. doi: 10.3354/meps334093

Mass, T., and Genin, A. (2008). Environmental versus intrinsic determination of colony symmetry in the coral Pocillopora verrucosa. *Mar. Ecol. Prog. Ser.* 369, 131–137. doi: 10.3354/meps07578

McFall-Ngai, M. (2007). Care for the community. *Nature* 445, 153–153. doi: 10.1038/445153a

Moberg, F., and Folke, C. (1999). Ecological goods and services of coral reef ecosystems. *Ecol. Econ.* 29, 215–233. doi: 10.1016/S0921-8009(99)00009-9

Mor Khalifa, G., Kahil, K., Erez, J., Kaplan Ashiri, I., Shimoni, E., Pinkas, I., et al. (2018). Characterization of unusual MgCa particles involved in the formation of foraminifera shells using a novel quantitative cryo SEM/EDS protocol. *Acta Biomater.* 77, 342–351. doi: 10.1016/J.ACTBIO.2018.07.026

Nir, O., Gruber, D. F., Shemesh, E., Glasser, E., and Tchernov, D. (2014). Seasonal mesophotic coral bleaching of *Stylophora pistillata* in the Northern Red Sea. *PLoS One* 9:e84968. doi: 10.1371/journal.pone.0084968

Oakley, C. A., and Davy, S. K. (2018). "Cell biology of coral bleaching," in *Coral Bleaching Ecological Studies*, eds M. van Oppen and J. Lough (Cham: Springer), 189–211. doi: 10.1007/978-3-319-75393-5-8

Ow, Y. X., and Todd, P. A. (2010). Light-induced morphological plasticity in the scleractinian coral goniastrea pectinata and its functional significance. *Coral Reefs* 29, 797–808. doi: 10.1007/s00338-010-0631-634

Parkinson, J. E., Baumgarten, S., Michell, C. T., Baums, I. B., LaJeunesse, T. C., and Voolstra, C. R. (2016). Gene expression variation resolves species and individual strains among coral-associated dinoflagellates within the genus symbiodinium. *Genome Biol. Evol.* 8, 665–680. doi: 10.1093/gbe/evw019

Poole, A. Z., Kitchen, S. A., and Weis, V. M. (2016). The role of complement in cnidarian-dinoflagellate symbiosis and immune challenge in the sea anemone Aiptasia pallida. *Front. Microbiol.* 7:519. doi: 10.3389/fmicb.2016.00519

Quast, C., Pruesse, E., Yilmaz, P., Gerken, J., Schweer, T., Yarza, P., et al. (2012). The SILVA ribosomal RNA gene database project: improved data processing and web-based tools. *Nucleic Acids Res.* 41, D590–D596. doi: 10.1093/nar/gks1219

Ralph, P., Gademann, R., Larkum, A., and Schreiber, U. (1999). In situ underwater measurements of photosynthetic activity of coral zooxanthellae and other reef-dwelling dinoflagellate endosymbionts. *Mar. Ecol. Prog. Ser.* 180, 139–147. doi: 10.3354/meps180139

Raz-Bahat, M., Douek, J., Moiseeva, E., Peters, E. C., and Rinkevich, B. (2017). The digestive system of the stony coral *Stylophora pistillata*. *Cell Tissue Res.* 368, 311–323. doi: 10.1007/s00441-016-2555-y

Reyes-Nivia, C., Diaz-Pulido, G., Kline, D., Guldberg, O.-H., and Dove, S. (2013). Ocean acidification and warming scenarios increase microbioerosion of coral skeletons. *Glob. Chang. Biol.* 19, 1919–1929. doi: 10.1111/gcb.12158

Rinkevich, B., and Loya, Y. (1979). The reproduction of the red Sea coral *Stylophora pistillata*. I. gonads and planulae. *Mar. Ecol. Prog. Ser.* 1, 133–144. doi: 10.3354/meps001133

Ritchie, R. J. (2008). Universal chlorophyll equations for estimating chlorophylls a, b, c, and d and total chlorophylls in natural assemblages of photosynthetic organisms using acetone, methanol, or ethanol solvents. *Photosynthetica* 46, 115–126. doi: 10.1007/s11099-008-0019-17

Roberts, C. M., Poloczanska, E. S., Heyward, A. J., Baird, A. H., and Pratchett, M. S. (1997). Connectivity and management of caribbean coral reefs. *Science* 278, 1454–1457. doi: 10.1126/science.278.5342.1454

Rodrigues, L. J., and Grottoli, A. G. (2007). Energy reserves and metabolism as indicators of coral recovery from bleaching. *Limnol. Oceanogr.* 52, 1874–1882. doi: 10.4319/lo.2007.52.5.1874

Saragosti, E., Tchernov, D., Katsir, A., and Shaked, Y. (2010). Extracellular production and degradation of superoxide in the coral *Stylophora pistillata* and cultured symbiodinium. *PLoS One* 5:e12508. doi: 10.1371/journal.pone.0012508

Schmittgen, T. D., and Livak, K. J. (2008). Analyzing real-time PCR data by the comparative C_T method. *Nat. Protoc.* 3, 1101–1108. doi: 10.1038/nprot.2008.73

Schneider, K., and Erez, J. (2006). The effect of carbonate chemistry on calcification and photosynthesis in the hermatypic coral acropora eurystoma. *Limnol. Oceanogr.* 51, 1284–1293. doi: 10.4319/lo.2006.51.3.1284

Schoepf, V., Grottoli, A. G., Levas, S. J., Aschaffenburg, M. D., Baumann, J. H., Matsui, Y., et al. (2015). Annual coral bleaching and the long-term recovery capacity of coral. *Proc Biol Sci.* 282, 20151887. doi: 10.1098/rspb.2015.1887

Schrameyer, V., Wangpraseurt, D., Hill, R., Kühl, M., Larkum, A. W. D., and Ralph, P. J. (2014). Light respiratory processes and gross photosynthesis in two scleractinian corals. *PLoS One* 9:e110814. doi: 10.1371/journal.pone.0110814

Serrano, E., Ribes, M., and Coma, R. (2017). Recurrent partial mortality events in winter shape the dynamics of the zooxanthellate coral oculina patagonica at high latitude in the mediterranean. *Coral Reefs* 36, 27–38. doi: 10.1007/s00338-016-1510-1514

Shenkar, N., Fine, M., and Loya, Y. (2005). Size matters: bleaching dynamics of the coral oculina patagonica. *Mar. Ecol. Prog. Ser.* 294, 181–188. doi: 10.3354/meps294181

Shoguchi, E., Shinzato, C., Kawashima, T., Gyoja, F., Mungpakdee, S., Koyanagi, R., et al. (2013). Draft assembly of the symbiodinium minutum nuclear genome reveals dinoflagellate gene structure. *Curr. Biol.* 23, 1399–1408. doi: 10.1016/J.CUB.2013.05.062

Smith-Unna, R., Boursnell, C., Patro, R., Hibberd, J. M., and Kelly, S. (2016). TransRate: reference-free quality assessment of de novo transcriptome assemblies. *Genome Res.* 26, 1134–1144. doi: 10.1101/gr.196469.115

Song, L., and Florea, L. (2015). Rcorrector: efficient and accurate error correction for Illumina RNA-seq reads. *Gigascience* 4:48. doi: 10.1186/s13742-015-0089-y

Stambler, N., and Dubinsky, Z. (2004). "Stress effects on metabolism and photosynthesis of hermatypic corals," in *Coral Health and Disease*, eds E. Rosenberg and Y. Loya (Berlin: Springer), 195–215. doi: 10.1007/978-3-662-06414-6-9

Stambler, N., and Dubinsky, Z. (2005). Corals as light collectors: an integrating sphere approach. *Coral Reefs* 24, 1–9. doi: 10.1007/s00338-004-0452-454

Stat, M., Carter, D., and Hoegh-Guldberg, O. (2006). The evolutionary history of symbiodinium and scleractinian hosts - Symbiosis, diversity, and the effect of climate change. *Perspect. Plant Ecol. Evol. Syst.* 8, 23–43. doi: 10.1016/J.PPEES.2006.04.001

Tambutté, É, Venn, A. A., Holcomb, M., Segonds, N., Techer, N., Zoccola, D., et al. (2015). Morphological plasticity of the coral skeleton under CO2-driven seawater acidification. *Nat. Commun.* 6:7368. doi: 10.1038/ncomms8368

Tchernov, D., Kvitt, H., Haramaty, L., Bibby, T. S., Gorbunov, M. Y., Rosenfeld, H., et al. (2011). Apoptosis and the selective survival of host animals following thermal bleaching in zooxanthellate corals. *Proc. Natl. Acad. Sci. U.S.A.* 108, 9905–9909. doi: 10.1073/pnas.1106924108

Titlyanov, E. A., Titlyanova, T. V., Yamazato, K., and van Woesik, R. (2001). Photo-acclimation dynamics of the coral *Stylophora pistillata* to low and extremely low light. *J. Exp. Mar. Bio. Ecol.* 263, 211–225. doi: 10.1016/S0022-098101003 09-304

Todd, P. A. (2008). Morphological plasticity in scleractinian corals. *Biol. Rev.* 83, 315–337. doi: 10.1111/j.1469-185X.2008.00045.x

Tolleter, D., Seneca, F. O., DeNofrio, J. C., Krediet, C. J., Palumbi, S. R., Pringle, J. R., et al. (2013). Coral bleaching independent of photosynthetic activity. *Curr. Biol.* 23, 1782–1786. doi: 10.1016/j.cub.2013.07.041

Trench, R. K. (1979). The cell biology of plant - Animal symbiosis. *Annu. Rev. Plant Physiol.* 30, 485–531. doi: 10.1146/annurev.pp.30.060179.002413

van Oppen, M. J. H., Gates, R. D., Blackall, L. L., Cantin, N., Chakravarti, L. J., Chan, W. Y., et al. (2017). Shifting paradigms in restoration of the world's coral reefs. *Glob. Chang. Biol.* 23, 3437–3448. doi: 10.1111/gcb.13647

van Oppen, M. J. H., and Lough, J. M. (eds) (2018). *Coral bleaching*. Cham: Springer International Publishing, doi: 10.1007/978-3-319-75393-5

Venn, A. A., Loram, J. E., and Douglas, A. E. (2008). Photosynthetic symbioses in animals. *J. Exp. Bot.* 59, 1069–1080. doi: 10.1093/jxb/erm328

Ye, J., Coulouris, G., Zaretskaya, I., Cutcutache, I., Rozen, S., and Madden, T. L. (2012). Primer-BLAST: a tool to design target-specific primers for polymerase chain reaction. *BMC Bioinformatics* 13:134. doi: 10.1186/1471-2105-13-134

Zhang, T., Diaz, J. M., Brighi, C., Parsons, R. J., McNally, S., Apprill, A., et al. (2016). Dark production of extracellular superoxide by the coral porites astreoides and representative symbionts. *Front. Mar. Sci.* 3:232. doi: 10.3389/fmars.2016.00232

Conflict of Interest: The authors declare that the research was conducted in the absence of any commercial or financial relationships that could be construed as a potential conflict of interest.

Copyright © 2019 Zaquin, Zaslansky, Pinkas and Mass. This is an open-access article distributed under the terms of the Creative Commons Attribution License (CC BY). The use, distribution or reproduction in other forums is permitted, provided the original author(s) and the copyright owner(s) are credited and that the original publication in this journal is cited, in accordance with accepted academic practice. No use, distribution or reproduction is permitted which does not comply with these terms.